

COMPARISON OF IMAGE ENHANCEMENT TECHNIQUES FOR RAPID PROCESSING OF POST FLOOD IMAGES

M. Harichandana¹, V. Sowmya¹, V.V. Sajithvariya¹, Ramesh Sivanpillai^{2,*}

¹ Center for Computational Engineering and Networking, Amrita School of Engineering, Amrita Vishwa Vidyapeetham, Coimbatore, TN 641 112, India - mhchandana@gmail.com, (v_sowmya, vv_sajithvariya)@cb.amrita.edu

² Wyoming GIS Center, University of Wyoming, Laramie, WY 82072, USA (ORCID: 0000-0003-3547-9464) – sivan@uwoyo.edu

KEY WORDS: Floods, Disaster response, Satellite images, Image contrast, Enhancement algorithms

ABSTRACT:

Satellite images are widely used for assessing the areal extent of flooded areas. However, presence of clouds and shadow limit the utility of these images. Numerous digital algorithms are available for enhancing such images and highlighting areas of interest. These algorithms range from simple to complex, and the time required to process these images also varies considerably. For disaster response, it is important to select an algorithm that can enhance the quality of the images in relatively short time. This study compared the relative performance of five traditional (Histogram Equalization, Local Histogram Equalization, Contrast Limited Adaptive Histogram Equalization, Gamma Correction, and Linear Contrast Stretch) algorithms for enhancing post-flood satellite images. Flood images with different levels of clouds and shadows were enhanced and output generated were evaluated in terms of processing time and quality as measured by Blind/Reference less Image Spatial Quality Evaluator (BRISQUE), a no-reference image quality metric. Findings from this study will provide valuable information to image analysts for selecting a suitable algorithm for rapidly processing post-flood satellite images.

1. INTRODUCTION

Satellite images provide invaluable information on post-disaster conditions to emergency management agencies. Images collected by remote sensors have been effective for evaluating post-disaster conditions (Brivio et al., 2002). Repeat coverage of the affected areas from multiple satellites enable us to track changes over time (Gianinetto et al., 2005), in hard to reach areas at a relatively lower cost, robustness, and with the availability of data preprocessing techniques (Kussul et al., 2008). Satellite-based remote sensing systems offer a bigger potential for assessment of disasters and in their management (Kerle, Oppenheimer, 2002).

Floods are one of the major disasters that impact natural- and built-ecosystems worldwide. Every year flooding events result in the loss of lives, and damages to infrastructure and natural ecosystems. Images collected by active (RADAR) and passive (optical) sensors (Figure 1) on-board satellites are used for mapping and monitoring the extent of floods and changes over time. Optical sensors are limited in terms of collecting data when thick clouds are present. RADAR signals can penetrate cloud cover and collect data on the aerial extent of floods. However, there are relatively more optical sensors than those that collect RADAR data. Hence more optical images are available for monitoring post-flood conditions.

The visual quality of many post-flood optical images can be poor due to factors such as presence of haze, aerosols, and thin clouds and associated shadows (Lee, Lin 2016; Luscombe, Hassan, 1993). Differences in the spectral reflectance from features such as water, forest, vegetation etc. result in poor quality (Singh et al., 2019). Presence of these factors limit the use of optical images for monitoring post-flood conditions.

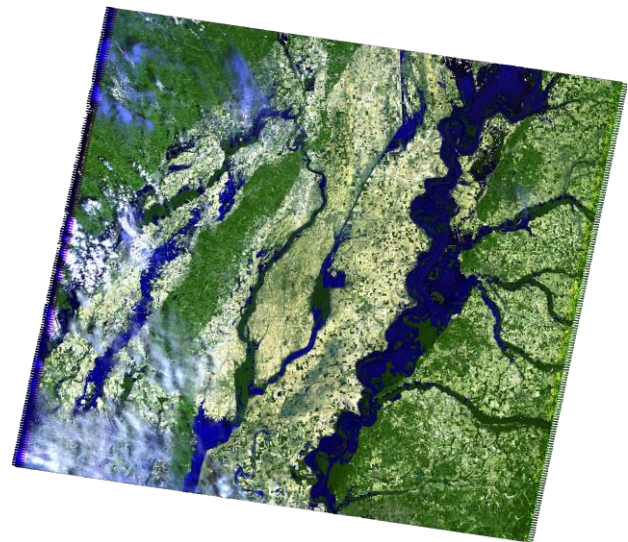


Figure 1. Landsat 5 Thematic Mapper acquired on 10 May 2011 shows the flooding in the Mississippi River, USA (Image credit: USGS/NASA)

Digital enhancement methods can be used to improve the quality of these optical images to extract useful information from them. Most of these methods focus on manipulating intensity and contrast, de-blurring, de-noising, and edge detection (Bidwai, Tuptewar, 2015). These digitally enhanced

* Corresponding author

images provide additional data to the emergency management agencies for planning rescue and recovery missions.

Numerous image enhancement methods such as Histogram Equalization (Stark, 2000), Linear Contrast Stretching (Gillespie, 1992), Brightness Preserving Bi-Histogram Equalization (Moniruzzaman et al., 2014), Local Histogram Equalization (Kim et al., 1998), Gamma Correction (Huang et al., 2016), Adaptive Histogram Equalization (Pizer et al., 1987), Contrast Limited Adaptive Histogram Equalization (Pizer et al. 1990), Minimum Mean Brightness Error Bi-histogram Equalization (Chen, Ramli, 2003), Dualistic Sub-image Histogram Equalization (Wang et al., 1999) are available for processing low visual quality images. These methods use either spatial or frequency domain for enhancing the quality of the images. To maximize the utility of poor-quality images, emergency management agencies have to enhance those using methods that will produce a quality output in relatively less time. The primary objective of this study was to evaluate the resultant image quality and associated processing time of five frequently used enhancement methods. Post-flood satellite data collected from actual flood events were used to test the performance of Histogram Equalization (HE), Local Histogram Equalization (LHE), Contrast Limited Adaptive Histogram Equalization (CLAHE), Gamma correction (GC), and Linear Contrast Stretch (LCS) methods.

The quality of enhanced images generated by these methods were evaluated using Blind/Reference less Image Spatial Quality Evaluator (BRISQUE) metric. This metric operates in the spatial domain and calculates the loss in naturalness of the image due to distortions by computing locally normalized luminance coefficients using statistics from the enhanced image (Mittal et al., 2012) Results from this study will provide valuable information to emergency management agencies or their partners to select appropriate enhancement methods that will increase the overall quality of the post-flood images in a relatively short amount of processing time.

2. MATERIALS AND METHODS

2.1 Post-flood satellite images

Seven scenes acquired by Landsat 5 Thematic Mapper and Landsat 8 Operational Land Imager were subset to generate 16 multispectral images. These images had poor visual quality due to the presence of thin clouds, haze, and aerosols (Figure 2).



Figure 2. Two of the sixteen post-flood Landsat images used for comparison of the image enhancement algorithms. All images had clouds and haze that reduced their contrast.

First, blue, green, and red bands from these multispectral images were combined to generate 18 true-color images. Next, green and two infrared bands were combined to generate 18 natural or false-color images, resulting in 36 images.

2.2 Image-enhancement methods

Five frequently used image enhancements were selected for this study. One of the criteria used for selecting is their availability in image processing and geospatial software. Brief description of each method is included in the following subsections. All images were processed in Python 3.6 installed in a Windows 10 computer with Intel core i5 (7th generation), 2.71 GHZ, 64-bit processor with 8 GB RAM. Time taken to process each image was recorded and later converted to seconds per megabytes.

2.2.1. Histogram Equalization (HE)

Histogram Equalization (HE) is a spatial domain-based enhancement method that increases the global contrast of an image. For a given input image, HE method automatically determines the transformation function based on the probability density function and maps the grey scale values in the input image to a uniform histogram which is widely spread throughout the available range of radiometric values. For an 8-bit image, the values will be spread from 0 (minimum) to 255 (maximum). Images enhanced by HE can be severe washed out effects due to saturation issues. Also, HE can ignore local details and might not preserve the brightness. Further details on HE method can be found in Stark (2000).

2.2.2. Local Histogram Equalization (LHE)

Local Histogram Equalization (LHE) method uses a sliding window and modifies the values of the central pixel based on the histogram of the subset area. LHE, also known as Adaptive HE, was proposed to overcome one of the limitations of HE method while relies on the histogram for computing the transformation function. The window is moved around the image in both horizontal and vertical direction and in every step the value of the central pixel is modified. A window size has been selected in order to generate an optimal enhanced image. In this study, five window sizes (8x8, 16x16, 32x32, 64x64, and 128x128) were tested. LHE method is computationally intensive and therefore time consuming. Also, LHE can lead to over amplification of noise in the relatively homogeneous areas of the image. Further details on LHE method can be found in Kim et al., (1998).

2.2.3. Contrast-Limited Adaptive Histogram Equalization (CLAHE)

CLAHE is a modification of the LHE method aimed to overcome the problem of over amplification of noise. In this method, the analyst must define a limit for clipping the local histogram and maximum enhancement factor. In the first step, the algorithm divides the input image into non overlapping blocks of equal size. In the second and final step, the algorithm clips the histogram for each block based on the user defined limit, and the cumulative density function is calculated for linearly mapping the pixel intensities. CLAHE method is also computationally intensive. Further details on CLAHE method can be found in Pizer et al. (1990). In this study, $1/8^{\text{th}}$ of the image height and weight was set as the window size. In this study, four clipping threshold values (0.01, 0.02, 0.03 and 0.09) were tested.

2.2.4. Linear Contrast Stretch (LCS)

LCS linearly stretches the contrast of an image by spreading the pixel intensity values over the entire dynamic range. The pixel values in low contrast images cover a limited range of intensity values. LCS stretches the intensity values over the entire range of the histogram. After LCS, bright areas in the image become brighter and the dark areas become darker. One of the disadvantages of assigning equal intensity values to both rarely and frequently occurring pixels, some important details might be lost. Also, LCS cannot improve the contrast if the pixel intensity values cover the entire available range. Further details on LCS method can be found in Gillespie (1992).

2.2.5. Gamma Correction (GC)

GC which is also known as Power Law Transform is a spatial domain contrast enhancement method where the value of each pixel in the input image is mapped to a new value based on a transformation function. The transformation function is based on scaling (c) and positive (γ) constants that are specified by the analyst. When γ values are set below 1, narrow range of dark input pixel values are transformed to a wide range of bright output values. When γ values are set above 1, the bright input pixel values are transformed to a narrow range of dark output values. Further details on GC method can be found in Huang et al. (2016). In this study, five potential γ values (0.1, 0.3, 0.5, 0.7, and 0.9) were tested. The value of c was chosen as 1.

2.3 Non-reference Evaluation Metric

Output images generated from each enhancement method was evaluated using the Blind/Reference less Image Spatial Quality Evaluator (BRISQUE). BRISQUE is an assessment metric that calculates the loss in naturalness of the image due to distortions (35). The value of BRISQUE score ranges between 0 and 100 and lower scores indicate better quality output image. Further details on BRISQUE can be found in Mittal et al. (2012).

3. RESULTS

3.1 Window size for LHE

BRISQUE scores of the output images generated with different window sizes are listed in Table 1. Output image generated with a window size of 128 x 128 pixels had the lowest BRISQUE score. Hence this window size was selected to process the rest of the images.

Window size	BRISQUE
8 x 8	43.41
16 x 16	30.84
32 x 32	29.73
64 x 64	30.06
128 x 128	26.98

Table 1. BRISQUE scores of the output images generated with Local Histogram Equalization algorithm using five different window sizes.

3.2 Threshold value for CLAHE

BRISQUE scores of the output images generated with different clipping threshold values are listed in Table 2. The output image generated with a clipping threshold of 0.03 had the lowest BRISQUE score of 27.48. Hence this clipping threshold value was selected for processing the rest of the images.

Clipping threshold	BRISQUE
0.01	30.87
0.02	30.86
0.03	27.48
0.09	28.23

Table 2. BRISQUE scores of the output images generated with Contrast-Limited Adaptive Histogram Equalization algorithm with four clipping threshold values.

As the threshold value increased, the contrast of the output image also increased. However, over enhancement problems were noticed when the clipping threshold value of 0.09 was selected.

3.3 Quality Assessment of Output Images

Based on the BRISQUE scores of the output generated from true color Landsat images (Table 3), no one enhancement method consistently outperformed the rest. The mean BRISQUE value for the LHE generated images were lower than those obtained for other enhancement methods (Table 3). BRISQUE scores of the output images generated by the GC method was highest in comparison to other methods.

Image	HE	LHE	CLAHE	LCS	GC
1	19.99	22.17	22.32	30.88	42.19
2	28.77	31.50	33.77	32.46	44.19
3	23.29	28.85	32.30	28.70	43.06
4	32.75	38.82	30.87	39.66	35.41
5	30.37	26.98	22.65	35.29	50.28
6	24.34	28.52	28.72	25.67	35.93
7	26.30	21.28	31.89	31.32	45.84
8	30.47	19.87	33.49	36.34	45.29
9	29.98	31.44	28.20	34.85	46.40
10	32.39	33.29	37.22	31.78	41.61
11	30.68	13.40	30.26	30.88	54.67
12	37.34	12.09	33.98	40.60	48.02
13	38.07	31.18	36.51	40.39	43.73
14	33.86	24.71	31.72	35.16	46.40
15	27.71	7.73	27.72	28.71	30.32
16	30.82	14.85	32.04	25.78	43.95
17	17.28	13.90	27.55	26.81	45.74
18	31.59	27.21	34.35	36.31	42.18
Mean	29.22	23.77	30.86	32.87	43.62
Std. Dev	5.26	8.37	4.00	4.63	5.40

Table 3. BRISQUE scores of the output generated from true color post-flood Landsat images using five enhancement algorithms. Lower BRISQUE score indicates higher output quality.

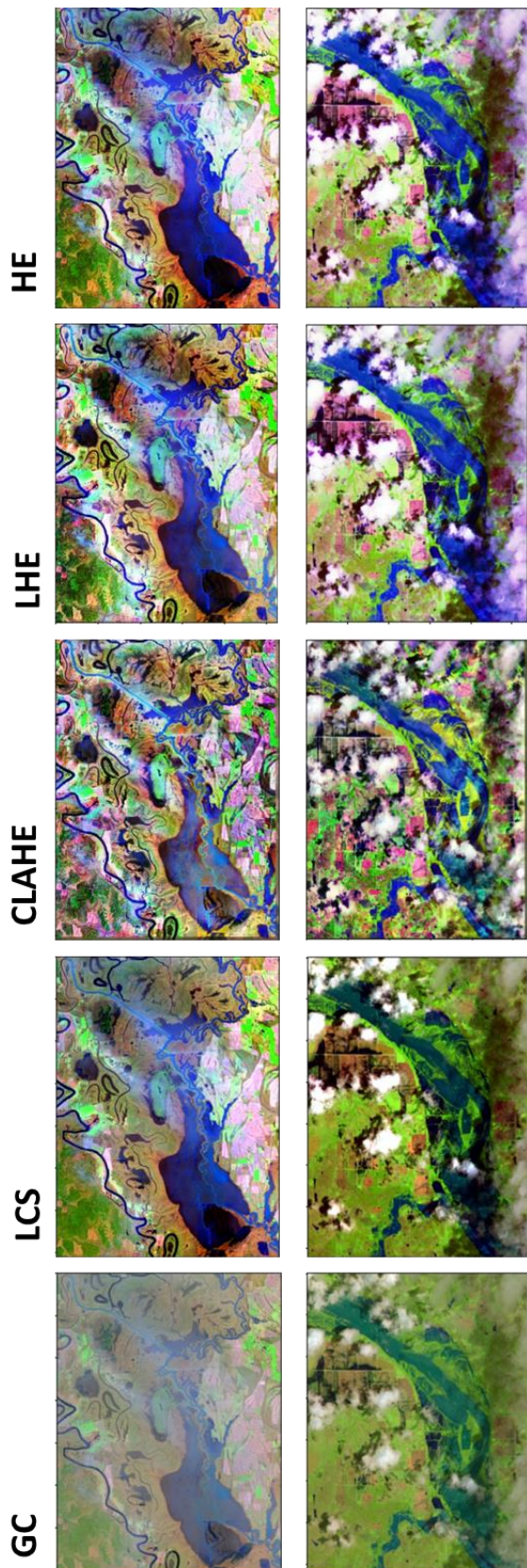


Figure 3. Output generated for two of the sixteen post-flood images using five image enhancement algorithms: Histogram Equalization (HE), Local Histogram Equalization (LHE), Contrast Limited Adaptive Histogram Equalization (CLAHE), Linear Contrast Stretch (LCS), and Gamma Correction (GC).

BRISQUE scores of the output generated from false color images (Table 4) showed a similar pattern. Like the true color images, the mean BRISQUE value for LHE generated images were lower than those obtained for other enhancement methods (Table 4). Among all methods, the output images generated by GC had the highest BRISQUE scores.

Image	HE	LHE	CLAHE	LCS	GC
1	23.02	36.23	24.62	31.96	32.47
2	29.54	17.66	30.57	22.35	36.94
3	30.97	21.61	30.70	29.27	33.62
4	21.86	21.21	24.08	31.26	25.11
5	28.48	23.17	16.13	31.86	39.76
6	24.15	19.13	20.53	18.75	27.28
7	20.79	26.36	30.60	27.50	44.46
8	14.60	22.32	30.98	25.54	36.95
9	30.83	29.76	18.25	28.32	33.92
10	31.55	21.14	33.07	22.17	35.09
11	16.99	13.86	28.06	29.59	40.31
12	23.94	19.26	25.61	32.03	50.83
13	31.00	23.47	29.78	37.25	44.34
14	22.34	23.49	33.39	25.56	46.23
15	27.52	6.88	25.66	21.51	28.52
16	25.19	25.26	25.18	23.65	27.40
17	21.59	25.99	14.65	25.64	32.56
18	33.83	32.59	39.62	32.68	42.87
Mean	25.46	22.74	26.75	27.61	36.59
Std Dev	5.19	6.44	6.28	4.69	7.07

Table 4. BRISQUE scores of the output generated from false color post-flood Landsat images using five enhancement algorithms. Lower BRISQUE scores indicate higher output quality.

Pair-wise comparison (one tailed, paired T-test) of the BRISQUE scores indicate that the output generated from each method was statistically different from the rest (Table 5). Output quality of LHE generated images are significantly different from those generated from other methods.

	LHE	LCS	CLAHE	GC
HE	< 0.01	< 0.01	N.S.	< 0.001
LHE		< 0.001	< 0.001	< 0.001
LCS			N.S.	< 0.001
CLAHE				< 0.001

Table 5. Probability values obtained from pair-wise comparison of the BRISUE scores of output images (n = 36) generated by five image enhancement techniques. N.S.: Not significant.

LHE divides the input image into blocks or tiles and redistributes the intensity level of the pixels by computing the histogram of each tile. Hence the overall contrast and edges of the image are enhanced even in the presence of noise, such as clouds (Figure 3). This resulted in lower BRISQUE scores and better overall performance by LHE method. However, this method is sensitive to the window size specified by the analyst.

Output from the HE method had the next lowest BRISQUE scores. Unlike LHE, this method does not require any input parameters such as specifying the window size. However, the pixels in the output images can be saturated due to the clipping effect, which results in loss of information. Hence the BRISQUE scores of HE were higher than that of LHE.

CLAHE method requires the analyst to specify the window size as well as a clip limit. The algorithm limits the contrast of the output image based on those values, which might lead to noise amplification and artifacts along the edges. Areas covered under thin clouds are not distinguishable (Figure). These factors resulted in higher average BRISQUE scores.

LCS increases the contrast of the input images by linearly spreading the histogram over the entire range. As a result, both frequently and rarely occurring pixels are assigned equal intensity values which results in poor quality output image (Figure). Hence the output generated by LCS had relatively higher BRISQUE scores than LHE, HE and CLAHE.

Among the five enhancement techniques, GC produced lowest quality images for all images. BRISQUE scores for 36 output images were higher than the corresponding scores obtained for the other 4 methods. The gamma value specified in this study did not spread the histogram over the entire dynamic data range. Based on the results obtained for the 36 images, LHE method generated higher quality images, followed by HE method.

Image	HE	LHE	CLAHE	LCS	GC
1	0.05	0.36	0.06	0.02	0.02
2	0.14	1.33	0.26	0.08	0.07
3	0.05	0.42	0.08	0.02	0.02
4	0.08	0.82	0.22	0.21	0.07
5	0.30	1.07	0.20	0.06	0.07
6	0.12	0.77	0.15	0.05	0.05
7	0.11	0.95	0.16	0.06	0.06
8	0.15	0.78	0.74	0.22	0.11
9	0.18	1.08	0.16	0.09	0.07
10	0.10	0.74	0.19	0.04	0.06
11	0.14	1.00	0.16	0.06	0.11
12	1.82	0.65	0.35	0.02	0.10
13	0.10	0.83	0.19	0.05	0.06
14	0.10	0.72	0.17	0.06	0.08
15	0.10	0.74	0.20	0.06	0.05
16	0.12	0.91	0.13	0.05	0.06
17	0.11	0.82	0.13	0.04	0.05
18	0.13	0.58	0.29	0.03	0.03
Mean	0.22	0.81	0.21	0.07	0.06
Std. Dev	0.39	0.23	0.14	0.05	0.03

Table 6: Time required (seconds/megabytes) by each enhancement algorithm (columns) to process the 18 true color images. LHE required most time in comparison to LCS and GC.

3.4 Processing Time

Standardized time taken (seconds/Megabytes) for processing each true color image was lower for GC and LCS in comparison to the other methods (Table 6). LHE which produced higher quality images, i.e., lower BRISQUE scores, needed most time to process the images.

Standardized time taken (seconds/Megabytes) for processing each false color image was lower for GC and LCS in comparison to the other methods (Table 7). Like the previous batch, LHE which produced higher false quality images, i.e., lower BRISQUE scores, needed more time to process the images.

Image	HE	LHE	CLAHE	LCS	GC
1	0.04	0.30	0.05	0.02	0.02
2	0.13	0.78	0.16	0.05	0.07
3	0.04	0.29	0.05	0.02	0.03
4	0.08	0.51	0.39	0.04	0.03
5	0.11	0.95	0.13	0.06	0.05
6	0.13	0.85	0.13	0.04	0.06
7	0.12	0.88	0.15	0.04	0.05
8	0.15	0.63	0.30	0.04	0.04
9	0.11	1.03	0.18	0.48	0.56
10	0.14	0.75	0.17	0.04	0.06
11	0.10	0.87	0.16	0.12	0.08
12	0.10	0.77	0.20	0.02	0.05
13	0.11	0.68	0.17	0.04	0.05
14	0.13	1.24	0.15	0.04	0.05
15	0.11	0.73	0.15	0.04	0.05
16	0.12	0.82	0.14	0.05	0.05
17	0.12	0.81	0.13	0.04	0.05
18	0.10	0.61	0.29	0.03	0.03
Mean	0.11	0.75	0.17	0.07	0.08
Std. Dev	0.02	0.23	0.07	0.10	0.11

Table 7: Time required (seconds/megabytes) by each enhancement algorithm (columns) to process the 18 false color images. LHE required most time in comparison to LCS and GC.

LHE method divides the input image into tiles and processes each one separately, it takes the most amount of time. Though the CLAHE method also divides the input image into tiles, it did not require the same amount of processing time. Time required by LHE to process images could be a limitation during emergency response, especially when the file size of the input image is large. Under these circumstances HE could be used for enhancing the post-flood satellite images. However, the quality of the output images generated by HE was lower than those generated by LHE. Further studies must process data collected by other remote sensing satellites for other regions with different characteristics.

4. CONCLUSIONS

Based on the BRISQUE scores of the output images, LHE algorithm will be suitable for enhancing post-flood images covered by thin-clouds and haze. There was no difference in quality of the output generated from the true color or false color images. However, LHE method needed most time to process the images.

If numerous images have to be rapidly processed, HE method could serve as the alternative method. The quality of the output generated from HE algorithm was slightly lower than those generated by the LHE algorithm.

LCS and GC algorithms needed relatively the least amount of time to process the images however their output quality was much lower. The output images generated for both true and false color images had higher BRISQUE scores.

CLAHE required relatively less time than LHE, the quality of the output images was lower due to the presence of artifacts. The methods that required relatively less processing time did not generate quality output.

ACKNOWLEDGEMENTS

Authors thank the US Geological Survey for providing Landsat data at no-cost and Dr. K.P. Soman, Head, Center for Computational Engineering and Networking at Amrita Vishwa Vidyapeetham (Deemed University) for his invaluable support.

REFERENCES

Bidwai, P., Tuptewar, D.J., 2015: Resolution and contrast enhancement techniques for grey level, color image and satellite image, *International Conference on Information Processing (ICIP), Pune*, 511-515, doi.org/10.1109/INFOP.2015.7489437.

Brivio, P.A., Colombo, R., Maggi, M., Tomasoni R., 2002: Integration of remote sensing data and GIS for accurate mapping of flooded areas. *International Journal of Remote Sensing* 23(3), 429-441. doi.org/10.1080/01431160010014729.

Chen, S., Ramli, A.R., 2003: Minimum mean brightness error bi-histogram equalization in contrast enhancement, *IEEE Transactions on Consumer Electronics*, 49(4), 1310-1319, doi.org/10.1109/TCE.2003.1261234.

Gianinetto, M., Villa, P., Lechi G., 2005: Postflood damage evaluation using Landsat TM and ETM+ data integrated with DEM. *IEEE Transactions on Geoscience and Remote Sensing*, 44(1), 236-243. doi.org/10.1109/TGRS.2005.859952.

Gillespie, A.R., 1992: Enhancement of multispectral thermal infrared images: Decorrelation contrast stretching. *Remote Sensing of Environment*, 42(4), 147-155. doi.org/10.1016/0034-4257(92)90098-5

Kerele, N., Oppenheimer, C., 2002: Satellite remote sensing as a tool in lahar disaster management. *Disasters*, 26(2): 140-160. doi.org/10.1111/1467-7717.00197.

Kussul, N., Shelestov, A., Skakun S., 2008: Grid system for flood extent extraction from satellite images. *Earth Science*

Informatics 1, 105-117 (2008). doi.org/10.1007/s12145-008-0014-3.

Huang, Z., Zhang, T., Li, Q., Fang, H., 2016: Adaptive gamma correction based on cumulative histogram for enhancing near-infrared images. *Infrared Physics & Technology*, 79, 2015-215. doi.org/10.1016/j.infrared.2016.11.001.

Kim, T.K., Paik, J.K., Kang, B.S., 1998: Contrast enhancement system using spatially adaptive histogram equalization with temporal filtering, *IEEE Transactions on Consumer Electronics*, 44 (1), 82-87, doi.org/10.1109/30.663733.

Lee, K., Lin C., 2016: Cloud detection of optical satellite images using support vector machine. *Int. Arch. Photogramm. Remote Sens.*, XLI-B7, 289-293. doi.org/10.5194/isprsarchives-XLI-B7-289-2016.

Luscombe, B.W., Hassan, H.M., 1993: Applying remote sensing technologies to natural disaster risk management: Implications for developmental investments. *Acta Astronautica*, 29(10-11), 871-876. doi.org/10.1016/0094-5765(93)90169-W.

Mittal, A., Moorthy, A.K., Bovik, A.C., 2012: No-Reference Image Quality Assessment in the Spatial Domain. *IEEE Transactions on Image Processing*, 21 (12), 4695-4708, doi.org/10.1109/TIP.2012.2214050.

Moniruzzaman, M., Shafuzzaman, M., Hossain, M.F., 2014: Brightness preserving Bi-histogram equalization using edge pixels information, *2013 International Conference on Electrical Information and Communication Technology (EICT)*, Khulna, 1-5, doi.org/10.1109/EICT.2014.6777872.

Pizer, S.M., Amburn, E.P., Austin, J.D., Cromartie, R., Geselowitz, A., Greer, T., Romeny, B.T., Zimmerman, J.B., Zuiderveld, K., 1987: Adaptive histogram equalization and its variations. *Computer Vision, Graphics, and Image Processing*, 39(3): 355-368. doi.org/10.1016/S0734-189X(87)80186-X.

Pizer, S.M., Johnston, R.E., Ericksen, J.P., Yankaskas, B.C., Muller, K.E., 1990: Contrast-Limited Adaptive Histogram Equalization: Speed and Effectiveness. Proceedings of the First Conference on Visualization in Biomedical Computing, Atlanta, GA, USA, 337-345. doi.org/10.1109/VBC.1990.109340.

Singh, H., Kumar, A., Balyan, L.K., Singh, G.K., 2019: A novel optimally weighted framework of piecewise gamma corrected fractional order masking for satellite image enhancement, *Computers & Electrical Engineering*, 75, 245-2661. doi.org/10.1016/j.compeleceng.2017.11.014.

Startk J.A., 2000: Adaptive image contrast enhancement using generalizations of histogram equalization, *IEEE Transactions on Image Processing*, 9(5), 889-896, doi.org/10.1109/83.841534.

Wang, Y., Chen, Q., Zhang, B., 1999: Image enhancement based on equal area dualistic sub-image histogram equalization method, *IEEE Transactions on Consumer Electronics*, 45(1), 68-75, doi.org/10.1109/30.754419.